

Lipid Modulation of Protein-Induced Membrane Domains as a Mechanism for Controlling Signal Transduction[†]

Anne Hinderliter,[‡] Rodney L. Biltonen,[§] and Paulo F. F. Almeida^{*,||}

Department of Pharmaceutical Sciences, North Dakota State University, Fargo, North Dakota 58105,

Departments of Pharmacology and of Biochemistry and Molecular Genetics, University of Virginia Health System, Charlottesville, Virginia 22908, and Department of Chemistry and Biochemistry, University of North Carolina—Wilmington, Wilmington, North Carolina 28403

Received December 30, 2003; Revised Manuscript Received February 26, 2004

ABSTRACT: The reason for the enormous lipid variety present in eukaryotic membranes remains largely an enigma. We suggest that its role is to provide an on–off switch for a signaling event at the membrane level. This is achieved through lipid–lipid interactions that convert membrane protein binding and association events into very cooperative processes while maintaining reversibility. We have previously shown [Hinderliter, A., et al. (2001) *Biochemistry* 40, 4181–4191] that thermodynamic linkage between an intrinsic tendency for lipid demixing and a preferential interaction of a protein with a specific lipid within the mixture leads to dramatic changes in lipid and protein domain formation. Here, we tested the hypothesis that small alterations in lipid chemical structure alter the magnitude of the net interaction free energy (ω_{AB}) between unlike lipids in a predictable manner, and that even very small changes in ω_{AB} lead to dramatic changes in bilayer organization when coupled with protein binding. We systematically varied the chemical structure of phosphatidylcholine (PC), in mixtures with a fixed phosphatidylserine (PS), by changing the PC acyl chain length and the degree of unsaturation, and examined domain formation upon addition of a peripheral protein, the synaptotagmin I C2A motif. Experimental excimer/monomer ratios (E/M) of pyrene-substituted lipids mimicking the PS were interpreted using Monte Carlo computer simulations. E/M is larger if the PC melting temperature is lower, suggesting that domain formation is a thermodynamic consequence of weak interactions between PC and PS. Consistent with our hypothesis, only very small changes in ω_{AB} were required for prediction of large changes in lipid and protein domain formation.

The membranes of eukaryotic organisms contain thousands of different lipid species (1). However, despite decades of work in cell membrane physiology and membrane biophysics (2), the reason for this lipid variety remains essentially an enigma (3, 4). The problem is to explain the need for phospholipid species that vary only slightly, such as the difference resulting from the addition of a double bond or a methylene group to the acyl chains.

Yet when the behavior of lipid mixtures is studied, it is found that small changes in the difference between lipid–lipid interactions can lead to dramatic changes in the lateral organization of the lipid bilayer (5, 6). The interaction energy between two lipids, A and B, in a bilayer may be substantial, but the net interaction energy (ω_{AB}),¹ defined by the difference between an A–B interaction and the average of A–A and B–B interactions [$\omega_{AB} = \epsilon_{AB} - (\epsilon_{AA} + \epsilon_{BB})/2$],

may be very small in comparison. If the net interaction energy is near zero, random mixing occurs. However, the magnitude of ω_{AB} is typically on the order of a few hundred calories per mole (5, 7–12). These are small energies compared to kT , offering an enormous plasticity in the possibilities for lipid lateral distributions on the membrane, which can be significantly varied by small structural changes in one or more lipid species. Further, if proteins exhibit preferential lipid interactions, then lipid clustering and protein–membrane interactions will be strongly coupled

¹ Abbreviations: POPC, 1-palmitoyl-2-oleoyl-*sn*-glycero-3-phosphocholine; di-14:1PC, 1,2-dimyristoyl-*sn*-glycero-3-phosphocholine; di-16:1PC, 1,2-dipalmitoyl-*sn*-glycero-3-phosphocholine; di-18:1PC, 1,2-dioleoyl-*sn*-glycero-3-phosphocholine; di-18:2PC, 1,2-dipetrolinoyl-*sn*-glycero-3-phosphocholine; di-18:3PC, dilinolenoyl-*sn*-glycero-3-phosphocholine; di-20:1PC, 1,2-dieicosenoyl-*sn*-glycero-3-phosphocholine; di-20:4PC, 1,2-diarachidonoyl-*sn*-glycero-3-phosphocholine; di-22:1PC, 1,2-dierucoyl-*sn*-glycero-3-phosphocholine; di-22:6PC, 1,2-didocosahexenoyl-*sn*-glycero-3-phosphocholine; di-24:1PC, 1,2-dinervonoyl-*sn*-glycero-3-phosphocholine; POPs, 1-palmitoyl-2-oleoyl-*sn*-glycero-3-phosphoserine; Pyr-PG, 1-hexadecanoyl-2-(1-pyrenedecanoyl)-*sn*-glycero-3-phosphoglycerol; NBD-DOPE, *N*-(7-nitrobenz-2-oxa-1,3-diazol-4-yl)-1,2-dioleoyl-*sn*-glycero-3-phosphoethanolamine; T_m , melting temperature; D , diffusion coefficient; E/M, excimer/monomer ratio; (E/M)₀, E/M in the absence of protein; ω_{AB} , net unlike nearest-neighbor interaction free energy; ϵ_{ij} , interaction free energy between lipids i and j ; ω_P , preferential protein–PS interaction free energy; ΔG° , protein–lipid (PC) interaction free energy.

[†] This work was supported, in part, by Grants GM59205 (R.L.B.) and GM64443 (A.H.) from the National Institutes of Health and by Grant EPS9874802 (A.H.) from the National Science Foundation.

* To whom correspondence should be addressed: Department of Chemistry and Biochemistry, University of North Carolina—Wilmington, Wilmington, NC 28403. E-mail: almeidap@uncw.edu. Phone: (910) 962-7300. Fax: (910) 962-3013.

[‡] North Dakota State University.

[§] University of Virginia Health System.

^{||} University of North Carolina–Wilmington.

thermodynamically. Thus, the possibility of achieving sensitive modulation of lipid domain composition and size, and associated protein compartmentalization on the membrane surface, exists.

We have previously reported that a POPC/POPS lipid mixture even in the fluid state exhibited an intrinsic tendency to demix (5, 13). Moreover, addition of the synaptotagmin I C2A motif would further drive the system to formation of larger lipid clusters. The C2A motif of synaptotagmin I (14) is a peripheral membrane binding protein with 128 amino acid residues. The C2 motif is found in numerous proteins involved in trafficking and signaling. The interaction between C2 domains from different proteins (14–18) with the membrane varies somewhat, but a common motif is a hydrophobic face around which a few positively charged amino acids are located. Because of this patch of basic residues, C2A preferentially interacts with anionic lipids. The binding of the synaptotagmin I C2A motif to lipid membranes has recently been studied by measurement of the relative positions of spin-label probes attached to the protein (18). The increase in the level of domain formation upon addition of C2A to PS/PC mixtures is a consequence of the thermodynamic linkage of an intrinsic tendency for lipid lateral heterogeneity with the preferential interaction of a protein with the acidic lipid (PS) within the mixture. The data upon which this conclusion was based were obtained by monitoring the excimer/monomer ratio (E/M) of a pyrene-labeled lipid and their interpretation using the results Monte Carlo simulations of a two-state lipid model. These results demonstrated that lipid and protein cluster average sizes are highly correlated and that changes in the cluster size distributions could be altered greatly by small changes in the net lipid–lipid interaction energy, ω_{AB} (5).

In this article, we move one step further. We test the hypothesis that changes in the chemical structure of one lipid in a binary pair will change ω_{AB} , leading to changes in the tendency of the lipid to cluster. Furthermore, because only small changes in ω_{AB} are required for large changes in lipid domain formation, small changes in lipid structure can, when coupled to protein binding, lead to dramatic changes in protein organization on the membrane surface. Lipid–lipid interactions could be used to convert membrane protein binding and association events into very cooperative processes while maintaining reversibility. This is exactly what is required for an on–off switch in a signaling event at the membrane level.

In this work, we use lipid chain length and degree of unsaturation as a means of changing the net lipid–lipid interaction energy and investigate its consequences for domain formation in the absence and presence of an externally added peripheral membrane protein. We use binary mixtures containing as the minor component (16 mol %) the acidic lipid 1-palmitoyl-2-oleoylphosphatidylserine (POPS or 16:0,18:1PS) and as the major component a phosphatidylcholine (PC) for which the acyl chains are varied in the following homologous series: di-14:1PC, di-16:1PC, di-18:1PC, di-20:1PC, di-22:1PC, and di-24:1PC. Also tested was our reference, 16:0,18:1PC (POPC), and a series in which the degree of unsaturation is varied: di-18:2PC, di-18:3PC, di-20:4PC, and di-22:6PC. All these lipids, with the possible exception of di-24:1PC, are in the fluid state at room temperature. In these mixtures, a small amount (4 mol %)

of a phosphatidylglycerol labeled with a pyrene fluorophore on the *sn*-1 acyl chain (Pyr-PG) is included for monitoring domain formation through an increase in the pyrene excimer/monomer emission ratio. This acidic lipid probe has previously been shown to be a close mimic of the POPS behavior; namely, it appears to cocluster with PS (5). This conclusion was based on the observation that only a single set of values for the thermodynamic parameters ΔG° , ω_P , and ω_{AB} used in the simulations was necessary to reproduce the experimental protein binding data and E/M curves as a function of protein concentration obtained with bilayers containing from 5 to 40 mol % PS. If the PG probe were not a good mimic of the PS lipid, then a single set of parameter values would not be sufficient to adequately reproduce the experimental data.

It has been suggested that one of the mechanisms leading to lateral domain formation is the mismatch between the hydrophobic lengths of lipids and integral membrane proteins (19–31). The same concept applies to the mismatch of two lipids with acyl chains of different lengths (32). If the lipids are aligned on the bilayer surface, a length mismatch results at the bilayer midplane (or vice versa). According to the hydrophobic mismatch concept, ω_{AB} should vary monotonically with the difference in acyl chain between two phospholipids in a binary lipid mixture. Thus, ω_{AB} should be large for the shorter lipids (di-14:1PC), reach a minimum at POPC, and increase again beyond that as the PC acyl chains become longer. We come to the conclusion that although hydrophobic mismatch may provide an important contribution to ω_{AB} , it is not the only factor. Rather, it appears that it is the strength of the van der Waals interactions established by the PC that determines the value of ω_{AB} .

MATERIALS AND METHODS

Materials. All lipids and NBD-DOPE were from Avanti Polar Lipids, Inc. (Birmingham, AL). The pyrene-acyl chain-labeled phospholipid, 1-hexadecanoyl-2-(1-pyrenedecanoyl)-*sn*-glycero-3-phosphoglycerol, ammonium salt (Pyr-PG or 16:0,10-Pyr-PG), was from Molecular Probes, Inc. (Eugene, OR). All were greater than 99% pure as determined by thin-layer chromatography (TLC). All other reagents were as described in ref 5.

Preparation of Solutions. Water was doubly distilled through glass. The primary standard phosphate solution in water was prepared from an analytical concentrate (J. T. Baker, Inc., Bricktown, NJ). The concentration of phospholipid stock solutions in chloroform was periodically determined by phosphorus analysis (as described in ref 5). All lipid stock solutions were stored in the dark, under an argon atmosphere, at -72°C . All buffers used in fluorescence spectroscopy studies were decalcified by passing the $2\times$ buffer, 4 mM MOPS, and 200 mM KCl (pH 7.5) over a Chelex column before dilution with ddH₂O. The terbium chloride hexahydrate, a stable hydrate, was prepared gravimetrically using a Mettler balance and hydrated in decalcified buffer (Molecular Probes, Inc.). The lyophilized protein was also prepared gravimetrically, and a Bradford assay confirmed the concentration.

Expression and Purification of Recombinant Proteins. Recombinant proteins were purified by glutathione–agarose affinity essentially as documented in ref 5. A pGEX-KG

plasmid encoding glutathione *S*-transferase in frame with the C2 motif nearest the transmembrane sequence of rat synaptotagmin I was transformed into the AB1899 strain of *Escherichia coli*. The purified C2 motif was exhaustively dialyzed against 0.5 mM ammonium bicarbonate (pH 7.5) and lyophilized. The lyophilized protein was hydrated in decalcified 2 mM MOPS and 100 mM KCl (pH 7.5).

Preparation of Large Unilamellar Vesicles (LUV). Mixtures of PC and PS were prepared by aliquotting stock solutions of lipid in chloroform into borosilicate culture tubes using gastight syringes (Hamilton Co., Reno, NV). Samples were dried to a thin film under a gentle stream of argon and dried briefly under a vacuum of less than 20 mTorr before being lyophilized from a benzene/methanol mixture (19:1, v/v) or left on the vacuum line overnight. Lipid was hydrated in the dark above its gel–fluid phase transition temperature with 2 mM MOPS and 100 mM KCl (pH 7.5) under argon. LUV were prepared by extruding 200 μ L of a 4 mM multilamellar vesicle (MLV) dispersion through a 0.1 μ m pore size polycarbonate filter (Costar Scientific Corp., Cambridge, MA) 31 times using a hand-held extruder (Avanti Polar Lipids, Inc.). The dispersion was maintained above its gel–fluid phase transition temperature throughout the extrusion process. LUV containing the fluorescence probe were used within 48 h of preparation. All other lipid samples were used within a few days. All hydrated lipid samples were stored in the dark under an argon atmosphere at room temperature.

Fluorescence Spectroscopy Experiments. Fluorescence measurements were taken on a SLM Aminco 8100 instrument. For pyrene emission experiments, the excitation wavelength was 344 nm and emission spectra were recorded. Excitation and emission monochromator band-passes were 1 and 8 nm, respectively. Fluorescence measurements were also performed on a Jobin Yvon-Spex Fluorolog-3. Pyrene excitation was at 344 nm, and emission spectra were recorded with correction for the lamp output. Excitation and emission monochromator band-passes were 0.6 and 4.0 nm, respectively. A plateau voltage of 950 V was used. All samples were stirred continuously in a Teflon-capped 300 μ L mini-fluorimeter cell (McCarthy Scientific, Fullerton, CA), and all spectra were collected after a 15 min incubation between additions. The C2 domain titrations were carried out with a total lipid concentration of 24 μ M. Previously, a total lipid concentration of 200 μ M had been used (Figure 6 of ref 5).

Diffusion Measurements. To examine lipid diffusion, multibilayer samples were prepared as described in ref 33. Briefly, the two lipid components were mixed with NBD-DOPE in a 3:10000 molar ratio in chloroform. The mixture was deposited in a hot, siliconized (Sigmacote, siliconizing solution, Sigma) microscope slide in an area of approximately 1 cm². The samples were hydrated with buffer by a hanging drop of MOPS buffer placed on a coverslip and allowed to equilibrate overnight in a water-saturated glass chamber, and then sealed with high-vacuum grease. Diffusion measurements were performed by fluorescence recovery after photobleaching (FRAP) with periodic pattern photobleaching (50 lines/in.), using a Zeiss Axiovert 35 microscope and the 488 nm line of an Innova 300-8 argon laser (34). The FRAP data were fitted to a single-exponential decay equation to extract the diffusion coefficient; $F(t) = F(\infty) + [F_0 - F(\infty)] \exp(-Da^2t)$, where t is time, $a = 2\pi/p$ (p is the stripe

period), D is the translational diffusion coefficient, F_0 and $F(\infty)$ are the fluorescence intensities immediately after and at very long times after the bleaching pulse, respectively.

Monte Carlo Simulations. Monte Carlo simulations were performed as described in detail previously (5) to aid in the quantitative interpretation of the E/M results. Estimates of the intrinsic equilibrium constant for binding of C2 to pure PC LUV and the Gibbs energy difference associated with the preferential interaction of C2 with PS lipids relative to that for PC lipids were obtained from experimental evaluation of the equilibrium constant for association of the C2 motif with lipid bilayers as a function of anionic lipid composition. The values derived previously were used; namely, the intrinsic interaction between the protein and a pure PC bilayer was ΔG° (−5 kcal/mol of protein), and the preferential interaction of the protein with a PS over a PC lipid, ω_p , was set equal to −1 kcal/mol of lipid. The lipid–lipid interactions are described by an unlike nearest-neighbor interaction parameter (free energy), ω_{AB} , which was varied depending on the lipid mixture. In our previous study (POPC/POPS), we found that an ω_{AB} of 240 cal/mol was adequate for describing the experimental observations. Here, the variation in the structure of one of the lipids, the PC, in the PC/POPS mixtures is reflected in a change in ω_{AB} , which should increase with increasing chain length mismatch between lipid pairs if physical mismatch and thermodynamic mismatch are highly correlated. Briefly, the simulations are performed on a 100 \times 100 triangular lattice, each site representing a lipid molecule. The proteins, when bound, are represented by a 19-site hexagon, the 12 peripheral sites being able to interact preferentially with PS. This model was proposed by us (5) on the basis of the fact that the C2 motif interacts with the membrane by a hydrophobic face around which a few positively charged amino acids are located (14–17). This model has recently been corroborated by distance estimates using spin-labels attached to different positions on the protein (18). Both lipid and protein diffusion on the membrane are allowed moves. Additionally, the protein is allowed to bind to and desorb from the membrane (lattice) reversibly. The system (lattice) is thus closed with respect to the lipids but open with respect to the protein. The Monte Carlo simulations used the Metropolis algorithm to decide between accepted and rejected trial moves. Typical simulations consisted of 1–6 million cycles [Monte Carlo steps (mcs)] following 100 equilibration mcs. The very long runs were required to sample all accessible states especially for those cases where the interaction parameter $\omega_{AB} > 300$ cal/mol because the system then begins to exhibit features of complete demixing (5, 35). This was particularly noticeable when the protein concentration was high.

RESULTS

Changes in the Pyrene E/M as a Function of Protein Addition and Lipid Chemical Structure. We have previously shown that an increase in the E/M of Pyr-PG (4 mol %) incorporated in an 80:16 POPC/POPS mixture is an experimental indication of clustering of PS and PG lipids in the PC matrix (5). The influence of the chemical structure of the PC component on apparent lipid domain formation was now investigated by examining its effect on the E/M of Pyr-PG included in several PC/POPS mixtures as a function of

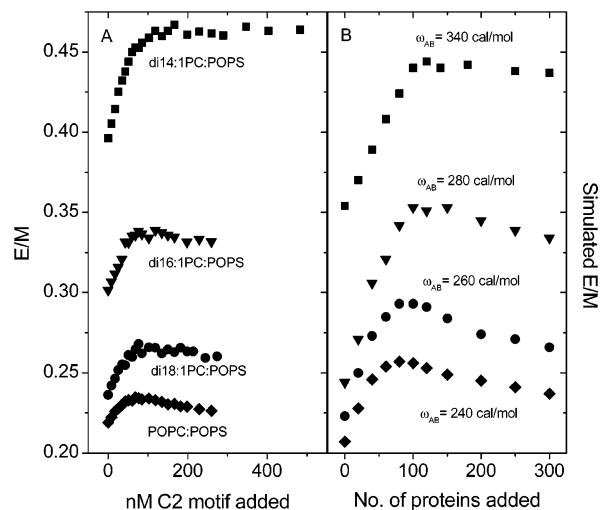


FIGURE 1: (A) Experimental E/M values for binary mixtures of PC and POPS as a function of C2 motif added. The measurements were taken at ambient temperature: POPC/POPS (◆), di-18:1PC/POPS (●), di-16:1PC/POPS (▼), and di-14:1PC/POPS (■). The total lipid concentration was 24 μ M for achieving protein saturation. In all cases, the total content of anionic lipid in LUV is 20% (16 mol % PS and 4 mol % Pyr-PG). (B) Computer-simulated values of E/M as a function of the number of proteins added to the system for various values of ω_{AB} : 240 (◆), 260 (●), 280 (▼), and 340 cal/mol (■). These were calculated from the average number of probe–probe contacts obtained from several simulations.

added C2 protein motif. As an example, the experimental E/M results obtained with large unilamellar vesicles composed of 16 mol % 16:0,18:1PS (POPS), 4 mol % Pyr-PG, and 80 mol % 16:0,18:1PC (POPC), di-18:1PC, di-16:1PC, or di-14:1PC are shown in Figure 1A. These results are similar to those previously reported with one important added feature. When compared to the values for our reference system, POPC/POPS, both the E/M in the absence of protein, $(E/M)_0$, and the maximal E/M obtained in the presence of protein change as the PC acyl chain is varied. In addition, $(E/M)_0$ and the maximal E/M appear to be highly correlated. Interpretation of these results within the context of our hypothesis that changing lipid chemical structure changes ω_{AB} suggests that acyl chain mismatch in binary lipid systems increases the propensity for both intrinsic and protein-induced lipid clustering. Indeed, intrinsic lipid demixing had already been observed in a mixture of Pyr-PC and PC with varying chain lengths, which was attributed to a hydrophobic mismatch (32).

As the C2 protein motif is added to the 80:16:4 PC/POPS/Pyr-PG mixtures, the E/M increases initially (Figure 1A). The overall amplitude of the change in the E/M upon protein addition increases with acyl chain mismatch: POPC < di-18:1PC < di-16:1PC < di-14:1PC. For the smaller mismatch cases (POPC and di-18:1PC), the E/M reaches a maximum and then decreases, whereas for the larger mismatch cases (di-16:1PC and di-14:1PC), the E/M seems to plateau and then remain essentially constant. We interpret the initial increase in the E/M as being indicative of the formation of domains rich in PS (and Pyr-PG) as a consequence of the protein preferentially binding to these types of lipids. As the protein concentration is increased beyond saturation of the anionic lipids, the PS lipid domains begin to dissipate if the acyl chain mismatch is small, but this does not appear to happen if the chain mismatch is large.

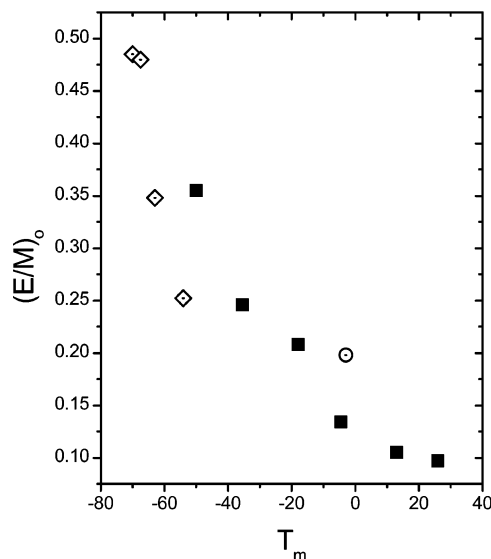


FIGURE 2: E/M measured for several 80:16:4 PC/POPS/Pyr-PG systems in the absence of protein $[(E/M)_0]$ as a function of the gel–fluid transition temperature of the PC: polyunsaturated acyl chain PCs (◇), monounsaturated acyl chain PCs (■), and POPC (○). The total lipid concentration was 200 μ M. All $(E/M)_0$ measurements were taken at ambient temperature. (See Table 1 for a listing of the PCs used and their respective T_m and D values.)

Table 1

	T_m^a (°C)	HC ^b (Å)	$D \pm SD$ ($\times 10^8$ cm ² /s) in 80:20 PC/POPS
di-14:1PC	−50 ^c	22.5	2.3 \pm 0.3
di-16:1PC	−35.5	26.0	3.0 \pm 0.8
di-18:1PC	−18	28.8	2.3 \pm 0.3
di-20:1PC	−4.5	32.5	2.3 \pm 0.5
di-22:1PC	13	36.4	2.0 \pm 0.4
di-24:1PC	26	40.5	2.0 \pm 0.5
di-18:2PC	−54	26.9	2.6 \pm 0.4
di-18:3PC	−63	26.3	2.1 \pm 0.5
di-20:4PC	−70	26.4	1.9 \pm 0.1
di-22:6PC	−67.5	26.4	2.0 \pm 0.3
POPC	−3.0	29.8	2.3 \pm 0.3

^a T_m values were rounded to the nearest half-degree (typical scatter is between 1 and 2 °C). Data taken from refs 37 and 38. ^b HC is the hydrophobic region, obtained from the peak-to-peak distance in electron density, which is roughly the position of the phosphates in the headgroup, by subtraction of 8 Å for the headgroup, which is consistent with the criteria of Wiener and White (39) (their estimate for the hydrophobic core of DOPC is 28.6 Å). Thickness values are the result of combination of data from refs 39–46. ^c By extrapolation from the 16:1–24:1 series.

$(E/M)_0$ was measured in a series of PC/POPS systems, in which the degree of unsaturation of the PC or its chain length (keeping one unsaturation per chain) was systematically varied. The results are shown in Figure 2, where $(E/M)_0$ is plotted as a function of the melting temperature of the PC. Table 1 lists the PC series, the thickness of their hydrophobic core, and their melting temperatures. First, we observe that there is a correlation between $(E/M)_0$ and the melting temperature of the PC. This is in agreement with published data obtained for mixtures of a Pyr-PC and the same series of PC (32). Second, as noted above, if the hydrophobic core of the PC is smaller than that of POPC (or POPS), that is, for di-14:1PC, di-16:1PC, and di-18:1PC, $(E/M)_0$ increases with acyl chain mismatch (Figure 3). This is consistent with the idea that chain length mismatch is directly proportional to ω_{AB} , which is reflected in an increase in $(E/M)_0$ (5).

However, for the lipid series in which the degree of unsaturation is varied, the dependence of $(E/M)_0$ on mismatch is much steeper than for the series in which the PC chain length is increased, indicating that some factor other than hydrophobic mismatch strongly influences lipid demixing for polyunsaturated lipids. Furthermore, for lipids with longer acyl chains (bilayer hydrophobic core larger than for POPC), the monotonic dependence of $(E/M)_0$ on hydrophobic mismatch breaks down: the changes in $(E/M)_0$ are small, which remains constant or even decreases, unlike the prediction from hydrophobic mismatch.

The only parameter that appears to correlate simply with the $(E/M)_0$ data for all phosphatidylcholines that were tested is the temperature of the main phase transition T_m of the PC (Figure 2). Specifically, the weaker the van der Waals interactions between the PC molecules (ϵ_{AA} becomes less negative), the larger the $(E/M)_0$ observed in mixtures of that PC and POPS (ω_{AB} becomes more positive).

To understand this result in terms of the lipid–lipid unlike nearest-neighbor interaction energy (ω_{AB}), we decompose ω_{AB} into a contribution from the chains and a contribution from the lipid headgroups:

$$\omega_{AB} = \omega_{AB}^c + \omega_{AB}^h \quad (1)$$

The headgroup contribution, ω_{AB}^h , is estimated to be 240 cal/mol (5) from the POPC/POPS mixture, where the chains are identical. We may now write the chain contribution as

$$\omega_{AB}^c = \epsilon_{AB}^c - (\epsilon_{AA}^c + \epsilon_{BB}^c)/2 \quad (2)$$

The dependence of ω_{AB}^c on the PC–PC acyl chain interactions is given by $d\omega_{AB}^c/d\epsilon_{AA}^c$, which we find experimentally to be positive (ω_{AB}^c must increase with the strength of the PC interactions because it decreases with the T_m). Differentiating eq 2, we have (note that ϵ_{BB}^c is independent of ϵ_{AA}^c)

$$d\omega_{AB}^c/d\epsilon_{AA}^c = d\epsilon_{AB}^c/d\epsilon_{AA}^c - 1/2 > 0 \quad (3)$$

Therefore

$$d\epsilon_{AB}^c/d\epsilon_{AA}^c > 1/2 \quad (4)$$

This means that as the strength of the van der Waals interactions between PC increases (a consequence of increasing chain length), the strength of the interactions between PC and PS also increases, at an absolute rate that is more than half as great.

We point out that the ϵ_{ij} parameters are, in general, free energies, not necessarily enthalpies. In particular, in the case presented here, the thermodynamic mismatch expressed by ω_{AB}^c probably contains a large entropic component, which results from the lipid chain structural fluctuations that are quenched when contact occurs between a lower- and higher-melting temperature phospholipid. Our data can thus be interpreted in a unified manner: $(E/M)_0$ simply reflects the change in the net lipid–lipid interaction energy, ω_{AB} . Acyl chain length mismatch is related to this value, but it is not the only factor in determining it. This is indicated by the results obtained with the polyunsaturated series and the long chain monounsaturated PCs, which are not explained by simple hydrophobic mismatch.

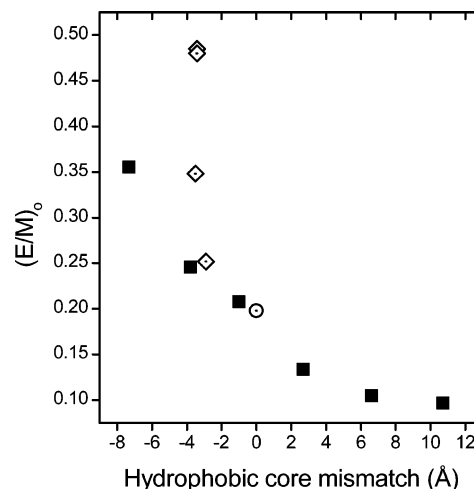


FIGURE 3: E/M_0 of various 80:16:4 PC/POPS/Pyr-PG systems as a function of the hydrophobic core mismatch between the PC and PS acyl chains. (See Table 1 for a listing of the hydrophobic core values.) Symbols are as in Figure 2: polyunsaturated acyl chain PCs (\diamond), monounsaturated acyl chain PCs (\blacksquare), and POPC (\circ).

Monte Carlo Simulations of Lipid Domain Formation. To gain a more quantitative understanding of the E/M experiments as a function of added protein, Monte Carlo simulations were performed. The membrane was represented by a two-dimensional triangular lattice, each site corresponding to a lipid. The lipids were allowed to move on the lattice by exchange with a nearest neighbor. The C2 motif protein was allowed to bind reversibly to and diffuse on the lattice, and was represented by a 19-site hexagon when bound. The values used for the interaction free energy of the C2 motif with a pure PC membrane (ΔG°) and the excess free energy for interaction with an anionic lipid (ω_p) were those previously determined for the POPC/POPS system: $\Delta G^\circ = -5$ kcal/mol of protein and $\omega_p = -1$ kcal/mol of lipid (5). The value of the unlike lipid–lipid interaction parameter ω_{AB} was varied between 240 and 340 cal/mol. As argued above, this parameter is expected to increase in mixtures with POPS as follows: POPC < di-18:1PC < di-16:1PC < di-14:1PC. We define a “simulated E/M” as the number of probe–probe contacts in the simulation. Using values for ω_{AB} of 240, 260, 280, and 340 kcal/mol seems to yield simulated E/M ratios (Figure 1B) that mimic the experimental variation of E/M as a function of added protein. The domain sizes of PS in the simulations show the same qualitative behavior (Figure 4). The increase in domain size upon protein addition is dramatic, especially if $\omega_{AB} > 300$ cal/mol. It is interesting to note that the Monte Carlo simulations reproduce not only the order and relative amplitude of the effects of adding protein but also the existence of a maximum in E/M for small ω_{AB} values and its absence for large ω_{AB} values. If there is a strong preference for like–like lipid interactions ($\omega_{AB} = 340$ kcal/mol), the protein does not seem to be able to cause PS lipid domain dissipation even at high protein concentrations.

Influence of Lipid Chain Length on Diffusion: Fluorescence Recovery after Photobleaching (FRAP). It could be argued that the dependence of $(E/M)_0$ on the chain length of the PC, which is the major component at 80 mol % in the mixtures that were studied, is merely a consequence of a decrease in the lateral diffusion coefficient (D). In fact, at a fixed temperature T , D is expected to decrease as the chain

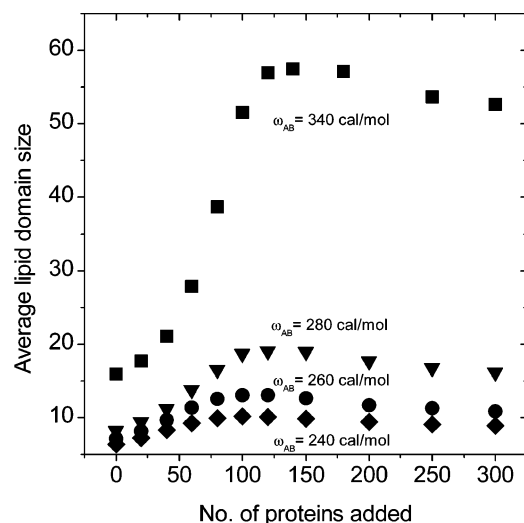


FIGURE 4: Average lipid domain size as a function of the number of proteins added to the system for various values of ω_{AB} : 240 (◆), 260 (●), 280 (▼), and 340 cal/mol (■). We have previously shown that the average protein domain size and the acidic lipid domain size are quantitatively correlated (5).

length of the PC increases, simply because of the dependence of the T_m on chain length. The dependence of D on T_m can be described by the equation $D = D_0 \exp\{-1/[\beta + \alpha(T - T_m)]\}$, where D_0 , α , and β are constants (36). Thus, at a fixed T , D decreases with T_m , resulting in a decrease in the collisional frequency and possibly in a smaller E/M. To examine whether the E/M results were due to changes in diffusion, D of the fluorescent lipid NBD-DOPE was measured using FRAP, at room temperature (ca. 25 °C) in PC/POPS mixtures containing the various PCs (80 mol %). For all lipid mixtures that were studied, D has similar values, typical for a fluid, L_α phase of phosphatidylcholines, even for an 80:20 di-24:1PC/POPS mixture, in which the T_m of the PC is 25.9 ± 2.5 °C (38). The results are summarized in Table 1. There appear to be no significant differences between these diffusion coefficients taken as a whole, and no monotonic correlation between D and $(E/M)_0$ is observed (Table 1). These results indicate that the changes in E/M as a function of acyl chain length mismatch are not a simple consequence of altered collisional frequency. For the polyunsaturated lipids, it appears that the values of D are smaller than for the monounsaturated series and they appear to follow a different dependence on temperature, which might reflect demixing of the PC/PS mixture, the NBD-PE probe, or both, but the differences are probably too small for a strong argument to be made. In conclusion, the experimental Pyr-PG E/M emission ratio is reporting primarily on the lateral organization of anionic lipids, that is, PS domain formation, and its change as a function of the lipid chemical structure and protein binding, not on diffusion effects.

DISCUSSION

We sought to test the hypothesis that changes in lipid chemical structure cause small changes in the net, unlike lipid-lipid interaction free energy (ω_{AB}). We further hypothesized that this can lead to dramatic changes in the intrinsic tendency for lipid domain formation, in protein-coupled domain formation, and in protein organization at the membrane surface. Our results show that if ω_{AB} is

sufficiently large, which means that the minor lipid component (PS) interacts unfavorably with the rest of the lipid, a dramatic increase in lipid domain size is obtained when a peripheral protein is added (Figure 4). This occurs even if the bilayer is in the fluid state. Formation of domains of lipid minor components may indeed play a crucial role in signal amplification by providing platforms for assembly of protein complexes.

Domain formation in the fluid state of lipid bilayer binary systems was studied using a combination of Pyr-PG fluorescence emission E/M ratios and Monte Carlo simulations of a two-state lattice model. The binary lipid mixtures were composed of 20 mol % negatively charged lipid [16 mol % POPS (16:0,18:1PS) and 4 mol % (16:0,10-pyrene)PG, a probe chosen to mimic the PS component] and 80 mol % PC. The chemical structure of the PS (and probe) was kept fixed, whereas the acyl chain length and the degree of unsaturation of the PC were varied, thus introducing a chain mismatch relative to POPS. The results can be briefly summarized as follows. For PC/POPS mixtures in which the PC hydrophobic length is increased in the series di-14:1PC, di-16:1PC, di-18:1PC, and POPC, $(E/M)_0$ increases (in the absence of protein) with chain mismatch. In the same series, addition of the C2 protein motif magnifies E/M in proportion to $(E/M)_0$. Both observations are well-explained by an increase in the unlike lipid-lipid nearest neighbor interaction energy (ω_{AB}) with acyl chain mismatch. However, if the degree of unsaturation is increased in the series di-18:2PC, di-18:3PC, di-20:4PC, and di-22:6PC, $(E/M)_0$ increases steeply while the size of the hydrophobic core (HC) of the PC essentially remains constant. (For all polyunsaturated lipids that were studied, $HC = 26.6 \pm 0.3$ Å; see Table 1 and references cited therein.) In addition, for PC/POPS mixtures in which the PC chain length is equal to or larger than that of POPS, in the series di-20:1PC, di-22:1PC, and di-24:1PC, $(E/M)_0$ does not increase with mismatch; if anything, it decreases.

Diffusion effects, if any, are small. For the PC series with monounsaturated acyl chains (di-xx:1PC), the lateral diffusion coefficient (D) follows the expected behavior as a function of T_m (Table 1). For the polyunsaturated lipids, it appears that the values of D are too small, which might reflect a heterogeneous bilayer in the corresponding mixtures with POPS. If so, this is in agreement with the conclusions drawn from the E/M results.

The only parameter that appears to correlate simply with the $(E/M)_0$ data for all phosphatidylcholines that were tested is the temperature of the main phase transition T_m of the PC (Figure 2). This indicates that the weaker the van der Waals interactions that the PC can establish, the larger the $(E/M)_0$ observed in mixtures of PC and POPS. Then, in the absence of protein, $(E/M)_0$ simply reflects the change in the net lipid-lipid interaction energy, ω_{AB} , with the chemical structure of the lipid. This is a consequence of the change in the magnitude of the van der Waals interactions between lipid chains. Acyl chain length mismatch may contribute to the value of ω_{AB} , but it is not the only factor, as indicated by results with the long chain monounsaturated and polyunsaturated series of PCs.

We have shown that extremely small net lipid-lipid interactions are all that is required to cause lipid demixing in a binary bilayer system. It is worth emphasizing that the

differences in ω_{AB} between any two lipid systems are only 100 cal/mol at most, but these small interactions can be coupled to the binding of a peripheral protein to lead to dramatic increases in the size the domains formed (Figure 4). The required protein–lipid preferential interactions are in fact also small, ~ 1 kcal/mol of free energy more favorable for a protein–PS contact than for a protein–PC contact. The implications of these observations cannot be overemphasized in terms of their consequences for the organization of biological membranes, in particular for the dynamical assembly of signal transduction complexes on the plasma membrane of eukaryotic cells.

The importance of lipid domains in membrane function has been suggested through both experimental and theoretical studies (47–54). The most intense recent work has revolved around the so-called lipid “rafts” and their existence in cell membranes (55–58). In its most restricted sense, rafts are protein/lipid domains rich in sphingomyelin, cholesterol, glycosphingolipids, glycosylphosphatidylinositol (GPI)-linked proteins, some transmembrane proteins, non-receptor tyrosine kinases, G-proteins, and transporters. Rafts have been implicated in a number of cell functions, including the facilitation of reactions between proteins and lipids that partition preferentially into the rafts, and sorting of components between different cell membranes (55). Some authors have used the term raft in a more general sense, as a synonym for domain. The same thermodynamic principles that determine domain formation in general apply to the formation of rafts, independent of semantics. Namely, rafts must form because of net unfavorable interactions between the raft components (sphingomyelin, cholesterol, glycosphingolipids, and proteins) and the nonraft components (unsaturated PC, mainly).

Lipid domains are normally perceived as static structures, although their dynamic nature has been stressed in the particular case of rafts (59, 60). Indeed, if the magnitudes of lipid–lipid interactions were sufficiently large, given the very large number of lipids involved in any membrane process, it is likely that formation of lipid domains would be essentially irreversible, leading to static or long-lived structures. However, in model bilayers, differences in interaction Gibbs energies between different lipid species are on the order of a few hundred calories per mole (5, 7–12). Because of cooperativity, these interactions are magnified, leading to domain formation, but since the energy barriers are small, the process remains reversible. The use of lipids to communicate membrane changes offers the possibility of cooperativity in the assembly of protein complexes on the membrane and of fine-tuning the combinations of proteins that will subsequently be assembled. In contrast, current views invoke separate and additive contributions from protein and lipid in assemblies stabilized by multiple protein interactions (61, 62).

We suggest that lipid diversity has a functional significance in signal transduction and propose the following hypothesis. Within signal transduction complexes, protein–protein, lipid–protein, and lipid–lipid interactions are small in magnitude. A favorable interaction of a protein with certain lipids induces accumulation of those lipids in the neighborhood of the protein. This change in local composition is sensed by other proteins, which are recruited to the domain and will induce further lipid reshuffling. The lipids interact

among themselves through contacts with six nearest neighbors, thus amplifying the original signal. This cooperative interaction leads to domain formation. Protein binding to a particular lipid is specific because of multiple interaction sites in the lipid headgroup (such as hydrogen bond donor and acceptor groups, charges, and methyl groups) and the multivalence of the protein surface, which interacts with multiple lipids. Because each of these interactions is small, the overall extent of binding becomes exquisitely sensitive to small changes in lipid structure, and it may change from weak to effectively irreversible with the addition of methylene groups or unsaturation to the acyl chains. This leads to a manifold of possible signaling assemblies. Two well-known mechanisms by which reaction rates on a membrane may be enhanced are a high protein concentration in domains and a reduction of dimensionality from a volume to a surface reaction (63). Here we propose that the assembly of protein complexes on the membrane may be regulated by small changes in lipid structure and that, because of cooperativity, those signaling complexes assemble and disassemble over a small concentration range of the components, ensuring an essentially on or off switch.

ACKNOWLEDGMENT

We thank Dr. Lukas Tamm for the use of his FRAP apparatus.

REFERENCES

1. Dowhan, W., and Bogdanov, M. (2002) Functional roles of lipids in membranes, in *Biochemistry of Lipids, Lipoproteins, and Membranes* (Vance, D. E., and Vance, J. E., Eds.) 4th ed., pp 1–35, Elsevier, Amsterdam.
2. Dowhan, W. (1997) Molecular basis for membrane phospholipid diversity: why are there so many lipids? *Annu. Rev. Biochem.* 66, 199–232.
3. Kinnunen, P. K. J. (1991) On the principles of functional ordering in biological membranes, *Chem. Phys. Lipids* 57, 375–399.
4. Mouritsen, O. G., and Andersen, O. S., Eds. (1998) In search of a new biomembrane model, *Biologiske Skrifter*, Vol. 49, pp 1–214, Munksgaard, Copenhagen.
5. Hinderliter, A., Almeida, P. F. F., Creutz, C. E., and Biltonen, R. L. (2001) Domain formation in a fluid mixed lipid bilayer modulated through binding of the C2 protein motif, *Biochemistry* 40, 4181–4191.
6. Risbo, J., Sperotto, M. M., and Mouritsen, O. G. (1995) Theory of phase equilibria and critical mixing points in binary lipid bilayers, *J. Chem. Phys.* 103, 3643–3656.
7. von Dreele, P. H. (1978) Estimation of lateral species separation from phase transitions in nonideal two-dimensional lipid mixtures, *Biochemistry* 17, 3939–3943.
8. Sugár, I. P., Biltonen, R. L., and Mitchard, N. (1994) Monte Carlo simulation of membranes: phase transition of small unilamellar dipalmitoylphosphatidylcholine vesicles, *Methods Enzymol.* 240, 569–593.
9. Sugár, I. P., Thompson, T. E., and Biltonen, R. L. (1999) Monte Carlo simulation of two-component bilayers: DMPC/DSPC mixtures, *Biophys. J.* 76, 2099–2100.
10. Jerala, R., Almeida, P. F. F., and Biltonen, R. L. (1996) Simulation of the gel-fluid transition in a membrane composed of lipids with two connected acyl chains: application of a dimer-move step, *Biophys. J.* 71, 609–615.
11. Vigmond, S. J., Dewa, T., and Regen, S. L. (1995) Nearest-neighbor recognition within a mixed phospholipid membrane: evidence for lateral heterogeneity, *J. Am. Chem. Soc.* 117, 7838–7839.
12. Dewa, T., Vigmond, S. J., and Regen, S. L. (1996) Lateral heterogeneity in fluid bilayers composed of saturated and unsaturated phospholipids, *J. Am. Chem. Soc.* 118, 3435–3440.

13. Huang, J., Swanson, J. E., Dibble, A. R. G., Hinderliter, A. K., and Feigenson, G. W. (1993) Nonideal mixing of phosphatidylserine and phosphatidylcholine in the fluid lamellar phase, *Biophys. J.* **64**, 413–425.
14. Shao, X., Fernandez, I., Sudhof, T. C., and Rizo, J. (1998) Solution structures of the Ca^{2+} -free and Ca^{2+} -bound C2A domain of synaptotagmin I: does Ca^{2+} induce a conformational change? *Biochemistry* **37**, 16106–16115.
15. Macedo-Ribeiro, S., Bode, W., Huber, R., Quinn-Allen, M. A., Kim, W., Ortel, T. L., Bourenkov, G. P., Bertunik, H. D., Stubbs, M. T., Kane, W. H., and Fuentes-Prior, P. (1999) Crystal structures of the membrane-binding C2 domain of human coagulation factor V, *Nature* **402**, 434–439.
16. Pratt, K. P., Shen, B. W., Tekeshima, K., Davie, E. W., Fujikawa, K., and Stoddard, B. L. (1999) Structure of the C2 domain of human factor VIII at 1.5 Å resolution, *Nature* **402**, 439–442.
17. Verdager, N., Corbalan-Garcia, S., Ochoa, W. F., Fite, I., and Gomez-Fernandez, J. C. (1999) Ca^{2+} bridges the C2 membrane-binding domain of protein kinase C α directly to phosphatidylserine, *EMBO J.* **18**, 6329–6338.
18. Frazier, A. A., Roller, C. R., Havelka, J. J., Hinderliter, A., and Cafiso, D. S. (2003) Membrane-bound orientation and position of the synaptotagmin I C2A domain by site-directed spin labeling, *Biochemistry* **42**, 96–105.
19. Mouritsen, O. G., and Bloom, M. (1984) Mattress model of lipid–protein interactions in membranes, *Biophys. J.* **46**, 141–153.
20. Fattal, D. R., and Ben-Shaul, A. (1993) A molecular model for lipid–protein interaction in membranes: the role of hydrophobic mismatch, *Biophys. J.* **65**, 1795–809.
21. Marsh, D. (1995) Specificity of lipid–protein interactions, in *Biomembranes* (Lee, A. G., Ed.) Vol. 1, pp 137–186, JAI Press, Greenwich, CT.
22. Nezil, F. A., and Bloom, M. (1992) Combined influence of cholesterol and synthetic amphiphilic peptides upon bilayer thickness in model membranes, *Biophys. J.* **61**, 1176–1183.
23. Ren, J., Lew, S., Wang, Z., and London, E. (1997) Transmembrane orientation of hydrophobic α -helices is regulated both by the relationship of helix length to bilayer thickness and by the cholesterol concentration, *Biochemistry* **36**, 10213–10220.
24. Ren, J., Lew, S., Wang, J., and London, E. (1999) Control of the transmembrane orientation and interhelical interactions within membranes by hydrophobic helix length, *Biochemistry* **38**, 5905–5912.
25. Webb, R. J., East, J. M., Sharma, R. P., and Lee, A. G. (1998) Hydrophobic mismatch and the incorporation of peptides into lipid bilayers: a possible mechanism for retention in the Golgi, *Biochemistry* **37**, 673–679.
26. Gil, T., Ipsen, J. H., Mouritsen, O. G., Sabra, M. C., Sperotto, M. M., and Zuckermann, M. J. (1998) Theoretical analysis of protein organization in lipid membranes, *Biochim. Biophys. Acta* **1376**, 245–266.
27. Harroun, T. A., Heller, W. T., Weiss, T. M., Yang, L., and Huang, H. W. (1999) Experimental evidence for hydrophobic matching and membrane-mediated interactions in lipid bilayers containing gramicidin, *Biophys. J.* **76**, 937–945.
28. O’Keefe, A. H., East, J. M., and Lee, A. G. (2000) Selectivity in lipid binding to the bacterial outer membrane protein OmpF, *Biophys. J.* **79**, 2066–2074.
29. Mall, S., Broadbridge, R., Sharma, R. P., Lee, A. G., and East, J. M. (2000) Effects of aromatic residues at the ends of transmembrane α -helices on helix interactions with lipid bilayers, *Biochemistry* **39**, 2071–2078.
30. Morein, S., Killian, J. A., and Sperotto, M. M. (2002) Characterization of the thermotropic behavior and lateral organization of lipid-peptide mixtures by a combined experimental and theoretical approach: effects of hydrophobic mismatch and role of flanking residues, *Biophys. J.* **82**, 1405–1417.
31. Morein, S., Koeppe, R. E., II, Lindblom, G., de Kruijff, B., and Killian, J. A. (2000) The effect of peptide/lipid hydrophobic mismatch on the phase behavior of model membranes mimicking the lipid composition in *Escherichia coli* membranes, *Biophys. J.* **78**, 2475–2485.
32. Lehtonen, J. Y., Holopainen, J. M., and Kinnunen, P. K. (1996) Evidence for the formation of microdomains in liquid crystalline large unilamellar vesicles caused by hydrophobic mismatch of the constituent phospholipids, *Biophys. J.* **70**, 1753–1760.
33. Almeida, P. F. F., Vaz, W. L. C., and Thompson, T. E. (1992) Lateral diffusion in the liquid phases of dimyristoylphosphatidylcholine/cholesterol lipid bilayers: a free volume analysis, *Biochemistry* **31**, 6739–6747.
34. Kalb, E., Frey, S., and Tamm, L. K. (1992) Formation of supported planar bilayers by fusion of vesicles to supported phospholipid monolayers, *Biochim. Biophys. Acta* **1103**, 307–316.
35. Heimburg, T., and Biltonen, R. L. (1996) A Monte Carlo study of protein-induced heat capacity changes and lipid-induced protein clustering, *Biophys. J.* **70**, 84–96.
36. Vaz, W. L., Clegg, R. M., and Hallmann, D. (1985) Translational diffusion of lipids in liquid crystalline phase phosphatidylcholine multibilayers. A comparison of experiment with theory, *Biochemistry* **24**, 781–786.
37. Cevc, G., Ed. (1993) *Phospholipids Handbook*, Marcel Dekker, New York.
38. Koynova, R., and Caffrey, M. (1998) Phases and phase transitions of the phosphatidylcholines, *Biochim. Biophys. Acta* **1376**, 91–145.
39. Wiener, M. C., and White, S. H. (1992) Structure of a fluid dioleoylphosphatidylcholine bilayer determined by joint refinement of X-ray and neutron diffraction data. III. Complete structure, *Biophys. J.* **61**, 437–447.
40. Lewis, B. A., and Engelman, D. M. (1983) Lipid bilayer thickness varies linearly with acyl chain length in fluid phosphatidylcholine vesicles, *J. Mol. Biol.* **166**, 211–217.
41. Petrache, H. I., Goulaev, N., Tristram-Nagle, S., Zhang, R., Suter, R. M., and Nagle, J. F. (1998) Interbilayer interaction from high-resolution X-ray scattering, *Phys. Rev. E* **57**, 7014–7024.
42. Petrache, H. I., Tristram-Nagle, S., and Nagle, J. F. (1998) Fluid phase structure of EPC and DMPC bilayers, *Chem. Phys. Lipids* **95**, 83–94.
43. Tristram-Nagle, S., Petrache, H. I., and Nagle, J. F. (1998) Structure and interactions of fully hydrated dioleoylphosphatidylcholine bilayers, *Biophys. J.* **75**, 917–925.
44. Petrache, H. I., Salmon, A., and Brown, M. F. (2001) Structural properties of docosahexaenoyl phospholipid bilayers investigated by solid-state ^2H NMR spectroscopy, *J. Am. Chem. Soc.* **123**, 12611–12622.
45. Olbrich, K., Rawicz, W., Needham, D., and Evans, E. (2000) Water Permeability and Mechanical Strength of Polyunsaturated Lipid Bilayers, *Biophys. J.* **79**, 321–327.
46. Huber, T., Rajamoorthi, K., Kurze, V. F., Beyer, K., and Brown, M. F. (2002) Structure of docosahexaenoic acid-containing phospholipid bilayers as studied by ^2H NMR and molecular dynamics simulations, *J. Am. Chem. Soc.* **124**, 298–309.
47. Edidin, M. (2003) The state of lipid rafts: from model membranes to cells, *Annu. Rev. Biophys. Biomol. Struct.* **32**, 257–283.
48. Anderson, R. G. W., and Jacobson, K. (2002) A role for lipid shells in targeting proteins to caveolae, rafts, and other lipid domains, *Science* **296**, 1821–1825.
49. Polozova, A., and Litman, B. L. (2000) Cholesterol dependent recruitment of di22:6-PC by a G protein-coupled receptor into lateral domains, *Biophys. J.* **79**, 2632–2643.
50. Saxton, M. J., and Jacobson, K. (1997) Single-particle tracking: application to membrane dynamics, *Annu. Rev. Biophys. Biomol. Struct.* **26**, 373–399.
51. Hinderliter, A. K., Dibble, A. R. G., Biltonen, R. L., and Sando, J. J. (1997) Activation of protein kinase C by coexisting diacylglycerol-enriched and diacylglycerol-poor lipid domains, *Biochemistry* **36**, 6141–6148.
52. Dibble, A. R. G., Hinderliter, A. K., Sando, J. J., and Biltonen, R. L. (1996) Lipid lateral heterogeneity in phosphatidylcholine/phosphatidylserine/diacylglycerol vesicles and its influence on protein kinase C activation, *Biophys. J.* **71**, 1877–1890.
53. Thompson, T. E., Sankaram, M. B., Biltonen, R. L., Marsh, D., and Vaz, W. L. C. (1995) Effects of domain structure on in-plane reactions and interactions, *Mol. Membr. Biol.* **12**, 157–162.
54. Melo, E. C., Lourtie, I. M., Sankaram, M. B., Thompson, T. E., and Vaz, W. L. C. (1992) Effects of domain connection and disconnection on the yield of in-plane bimolecular reactions in membranes, *Biophys. J.* **63**, 1506–1512.
55. Simons, K., and Ikonen, E. (1997) Functional rafts in cell membranes, *Nature* **387**, 569–572.
56. Ahmed, S. N., Brown, D. A., and London, E. (1997) On the origin of sphingolipid/cholesterol-rich detergent-insoluble cell membranes: physiological concentrations of cholesterol and sphingolipid induce formation of a detergent-insoluble, liquid-ordered lipid phase in model membranes, *Biochemistry* **36**, 10944–10953.

57. Dietrich, C., Bagatolli, L. A., Volovyk, Z. N., Thompson, N. L., Levi, M., Jacobson, K., and Gratton, E. (2001) Lipid rafts reconstituted in model membranes, *Biophys. J.* 80, 1417–1428.
58. Heerklotz, H. (2002) Triton promotes domain formation in lipid raft mixtures, *Biophys. J.* 83, 2693–2701.
59. Young, R. M., Holowka, D., and Baird, B. (2003) A lipid raft environment enhances Lyn kinase activity by protecting the active site tyrosine from dephosphorylation, *J. Biol. Chem.* 278, 20746–20752.
60. Rietveld, A., and Simons, K. (1998) The differential miscibility of lipids as the basis for the formation of functional membrane rafts, *Biochim. Biophys. Acta* 1376, 467–479.
61. Harder, T. (2003) Formation of functional cell membrane domains: the interplay of lipid- and protein-mediated interactions, *Philos. Trans. R. Soc. London, Ser. B* 358, 863–868.
62. Pawson, T., and Nash, P. (2003) Assembly of cell regulatory systems through protein interaction domains, *Science* 300, 445–452.
63. Adam, G., and Delbrück, M. (1968) Reduction of dimensionality in biological diffusion processes, in *Structural Chemistry and Molecular Biology* (Rich, A., and Davidson, N., Eds.) pp 198–215, W. H. Freeman and Co., San Francisco.

BI036334T